# GISMO: A 2-Millimeter Bolometer Camera for the IRAM 30 m Telescope

Johannes G. Staguhn[a,b], Dominic J. Benford[a] Christine A. Allen[a], S. Harvey Moseley[a], Elmer H. Sharp[a,c], Troy J. Ames[a], Walter Brunswig[d], David T. Chuss[a], Eli Dwek[a], Stephen F. Maher[a,b], Catherine T. Marx[a], Timothy M. Miller[a,e], Santiago Navarro[d] Edward J. Wollack[a]

[a]NASA/Goddard Space Flight Center, Greenbelt, MD 20771, USA;
[b]SSAI, 10210 Greenbelt Rd., Lanham, MD 20706, USA;
[c]GST, 7855 Walker Drive, Suite 200, Greenbelt, MD 20770, USA;
[d] IRAM, Avenida Divina Pastora, 7, Nucleo Central, E 18012 Granada, Spain;
[e]QSS, 4500 Forbes Blvd., Lanham, MD 20706, USA

## ABSTRACT

We are building a bolometer camera (the Goddard-Iram Superconducting 2-Millimeter Observer, GISMO) for operation in the 2 mm atmospheric window to be used at the IRAM 30 m telescope. The instrument uses a 8x16 planar array of multiplexed TES bolometers which incorporates our newly designed Backshort Under Grid (BUG) architecture. Due to the size and sensitivity of the detector array (the NEP of the detectors is $4 \times 10^{-17}$ W/$\sqrt{\text{Hz}}$), this instrument will be unique in that it will be capable of providing significantly greater imaging sensitivity and mapping speed at this wavelength than has previously been possible. The major scientific driver for this instrument is to provide the IRAM 30 m telescope with the capability to rapidly observe galactic and extragalactic dust emission, in particular from high-z ULIRGs and quasars, even in the summer season. The 2 mm spectral range provides a unique window to observe the earliest active dusty galaxies in the universe and is well suited to better confine the star formation rate in these objects. The instrument will fill in the SEDs of high redshift galaxies at the Rayleigh-Jeans part of the dust emission spectrum, even at the highest redshifts. The observational efficiency of a 2 mm camera with respect to bolometer cameras operating at shorter wavelengths increases for objects at redshifts beyond $z \sim 1$ and is most efficient at the highest redshifts, at the time when the first stars were re-ionizing the universe. Our models predict that at this wavelength one out of four serendipitously detected galaxies will be at a redshift of $z > 6.5$.

**Keywords:** superconducting bolometers, bolometer cameras, high redshift universe

## 1. BACKGROUND

A key observational tool in the study of the evolution of the universe out to cosmological distances is to observe the (redshifted) thermal emission from interstellar dust in galaxies. The most distant astronomical objects known to date are luminous, dusty galaxies at redshifts $z \sim 6$, a time when the universe was less than one Gyears old. This is the epoch at which the reionization of the universe was still not completed. These dusty galaxies all experience a phase of violent star formation and a large number of them are confirmed to host luminous active nuclei known as quasars. One of the major scientific questions in the context of understanding the formation of structure in the universe is the question about the physics of the formation of these galaxies. It appears that a clue to understanding the formation of these galaxies is a better understanding of the relationship between the star formation and quasar activity with their corresponding feedback mechanisms in these objects. The bulk of the total luminosity in these dusty galaxies is redshifted into the millimeter regime and therefore can be efficiently observed at these wavelengths.

Further author information: (Send correspondence to Johannes Staguhn)
E-mail: staguhn@gsfc.nasa.gov, Telephone: +1 301 286 7840

## 2. GISMO: A 2 MM BOLOMETER CAMERA FOR THE IRAM 30 M TELESCOPE

At the NASA Goddard Space Flight Center we are now building the bolometer camera GISMO (the Goddard IRAM Superconducting 2-Millimeter Observer) which is optimized for operating in the 2 mm atmospheric window. We have been given an opportunity to operate the instrument on the IRAM 30 m telescope on Pico Veleta in Spain[1]. The instrument is primarily aimed at surveying the first dusty galaxies in the universe. The camera is built around an 8x16 pixel array of 2 mm, close-packed superconducting Transition Edge Sensor (TES) bolometers which will be described in more detail in the following chapter.

**Sky parameters for Pico Veleta**

Average winter atmosphere:
150 GHz: sky emissivity 0.1, sky noise $9 \times 10^{-17}$ W/$\sqrt{\text{Hz}}$
NEFD: 7 mJy/sqrt(Hz)
250 GHz: sky emissivity 0.2 sky noise $2.2 \times 10^{-16}$ W/$\sqrt{\text{Hz}}$
NEFD: 20 mJy/sqrt(Hz)

Average summer atmosphere:
150 GHz: sky emissivity 0.2, sky noise $1.6 \times 10^{-16}$ W/$\sqrt{\text{Hz}}$
NEFD: 12 mJy/sqrt(Hz)
250 GHz: sky emissivity 0.4 sky noise $4.0 \times 10^{-16}$ W/$\sqrt{\text{Hz}}$
NEFD: 46 mJy/sqrt(Hz)

Table 1. Typical winter- and summer sky background at Pico Veleta for a $\lambda/D$ sampling array with 20% bandwidth, observing in on-off mode at 50 degrees elevation. The following efficiencies were assumed: Optical throughput 0.5; detector 0.8; telescope efficiencies are from the 30 m users manual[2].

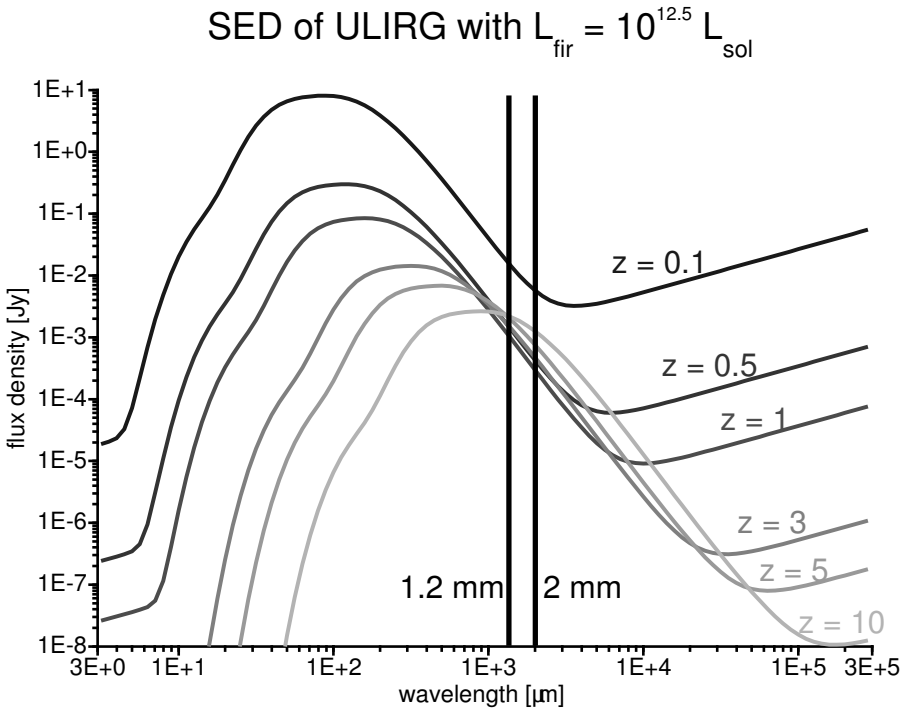


**Figure 1.** Model SED of an ULIRG with $L_{FIR} = 10^{12.5} L_{\odot}$ at different redshifts.

The 2 mm spectral range provides a unique low background window through the earth's atmosphere (see Table 1 which shows sky parameters for Pico Veleta). However, in order to obtain close to sky background limited

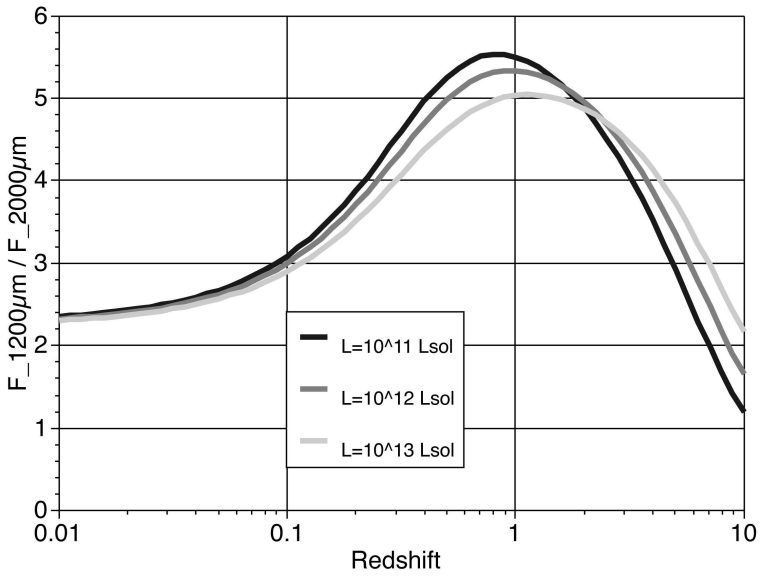


**Figure 2.** 1.2 mm over 2 mm color versus redshift for template ULIRG SEDs with three different luminosities as indicated.

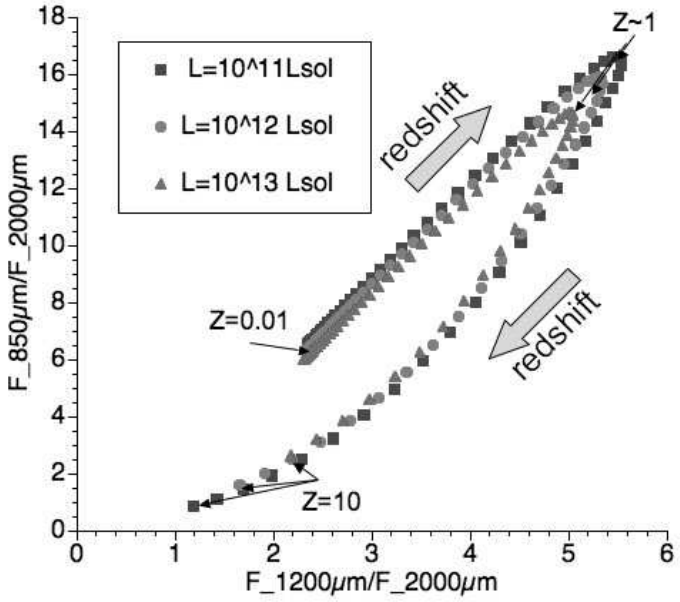


**Figure 3.** 2.0, 1.2, 0.8 mm color-color plot for three template galaxies. The color degeneracies of two color ratios (Fig. 2) are not present.

performance for a bolometer camera with 20% bandwidth operating at 2 mm wavelength, detectors with a noise equivalent power (NEP) of $\sim 4 \times 10^{-17}$ W/$\sqrt{\text{Hz}}$ or better are required. A camera which achieves this sensitivity then allows efficient observations of the earliest active dusty galaxies in the universe. Continuum measurements of galaxies at this wavelength are well suited to determine the star formation rate and the total energy output in these objects (for a review see e.g. [3]). Observations with GISMO will complement existing SEDs of high redshift galaxies at the Rayleigh-Jeans part of the dust emission spectrum, even at the highest redshifts (Figure 1). In particular at redshifts of $z > 5$ sky background limited bolometric observations at 2 mm are highly efficient

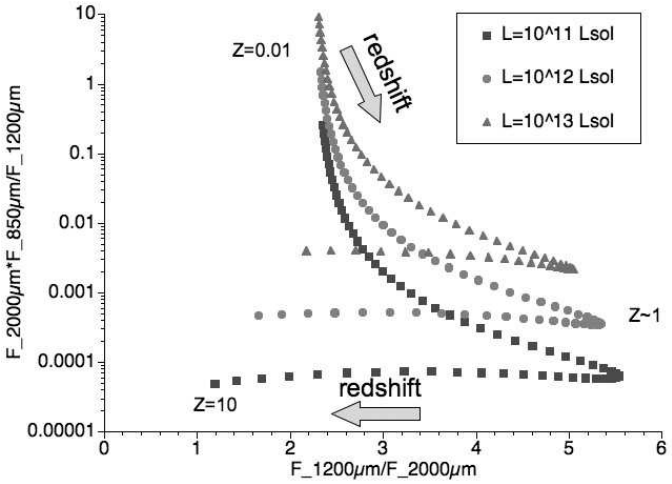


**Figure 4.** Another color-color display for the template galaxies shown in Fig. 2. This representation can be well used to determine the absolute luminosities of galaxies with $z > 1$.

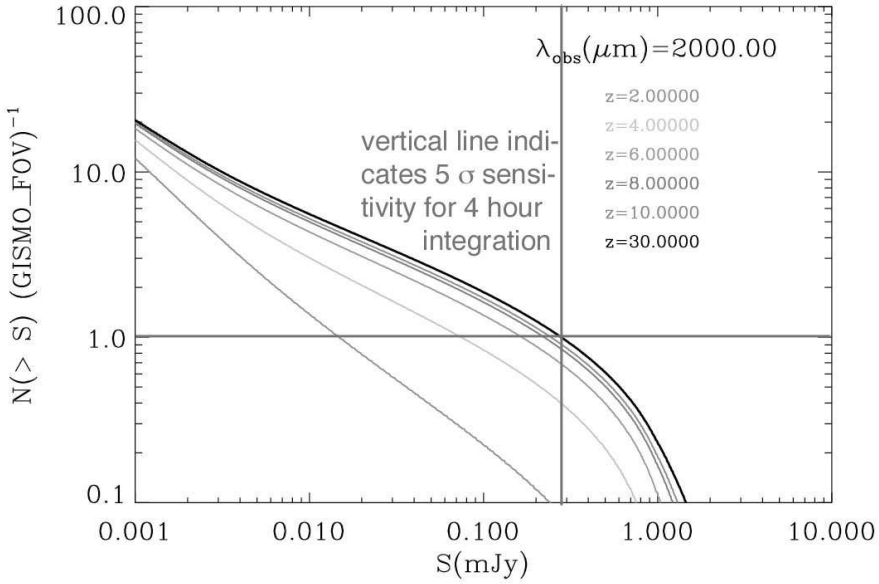


**Figure 5.** $N > S$ number counts versus flux for the instantaneous sky coverage of the GISMO instrument (4 arcmin x 2 arcmin). The curves shown are the *cumulative* values of $N > S$ up to the respective redshift.The confusion limits becomes important at 0.03 sources per beam or 4 sources per GISMO field of view (FOV)). The vertical line indicates the flux level (270$\mu$Jy) at which one source will be present in GISMO's FOV. In order to detect this source with a significance of 5$\sigma$, an integration time of 4 hours under good, but not excellent, winter conditions at Pico Veleta will be required. Our model predicts that one out of 4 blank field detections will be at a redshift $z > 6.5$.

as compared to observations at shorter (sub)millimeter wavelengths. Figure 2 demonstrates this by showing a plot of the 1.3mm/2mm flux ratio versus redshift for template ULIRGS with luminosities ranging between $L_{FIR} = 10^{11} L_{\odot}$ and $L_{FIR} = 10^{13} L_{\odot}$ . With GISMO operating at 2 mm wavelength, three atmospherical windows will be available for efficient continuum observations of the high-$z$ universe (2mm: GISMO, 1.2 mm: MAMBO[4], Bolocam[5], and 0.8 mm: SCUBA[6], and soon SCUBA-2 [7]). With the availability of three (sub)millimeter colors

the accuracy in the determination of photometric redshifts and absolute luminosities for those objects will be improved: Figs. 3 and 4 show 3-color plots for a number of templates, which demonstrate this. GISMO's pixel separation of 2 mm corresponds to an angular separation of 14″ on the sky, or $0.9\lambda/D$ (only slightly beam oversampled) at 2 mm wavelength and the telescope diameter of 30 m . With this spatial sampling GISMO will be very efficient at detecting sources serendipitously in large sky surveys, while the capability for diffraction limited observations is preserved[8]. Dithering will be used to recover the full angular resolution provided by the telescope. Fig. 5 shows our model predictions for the cumulative dark sky galaxy number counts versus flux for GISMO. Using the sensitivity numbers shown in Table 1 we find that we expect one 5 $\sigma$ galaxy detection on the blank sky in 4 hours of observing time, with the probability of 1 in 4 that it is at a redshift $z > 6.5$. Considering the current redshift "record" of $z = 6.4$ [9] this demonstrates the power of the instrument in surveying the high redshift universe. Other scientific projects for GISMO include – but are far from being limited to – large scale surveys of dust in protostellar clouds and galactic and extragalactic star forming regions.

## 3. DETECTORS: THE BACKSHORT-UNDER-GRID (BUG) ARRAY

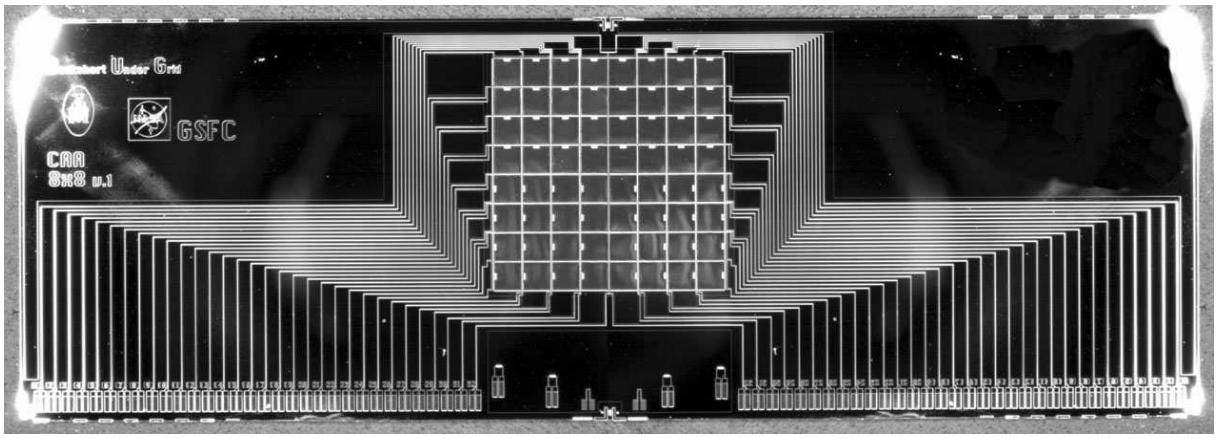


**Figure 6.** Image of an 8x8 planar BUG array. The array used in GISMO will have 8x16 pixels.

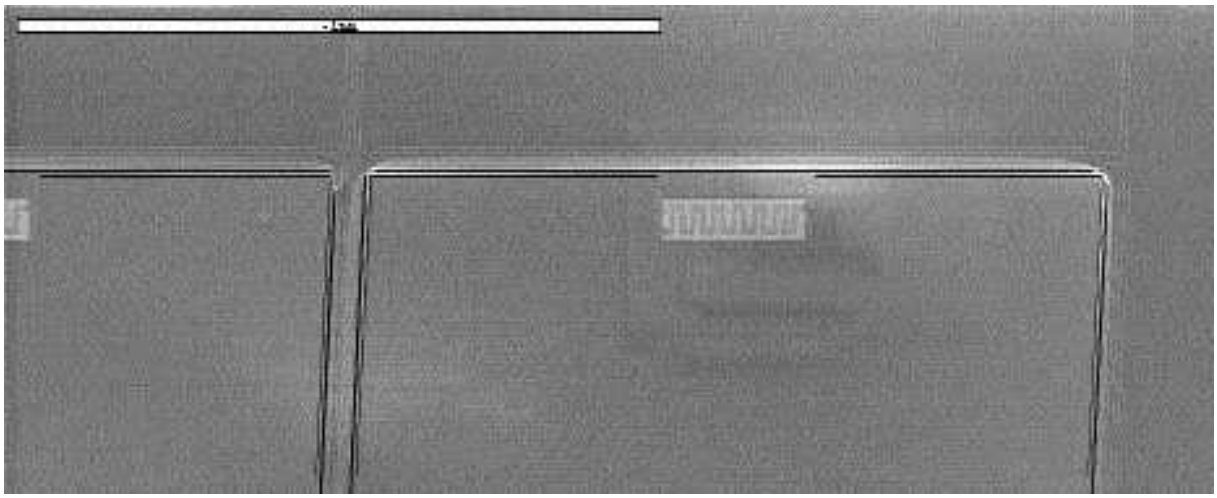

**Figure 7.** Photograph showing part of one pixel of the BUG array in detail. The TES sensor with its meandering Zebra normal metal layer can be seen near the top center on the pixel.

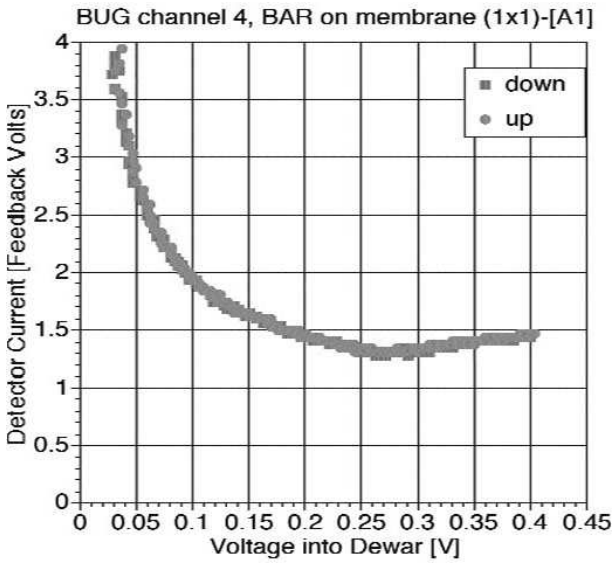


**Figure 8.** A representative I-V curve of a TES on a BUG pixel. Note that there is an arbitrary offset in the feedback current.

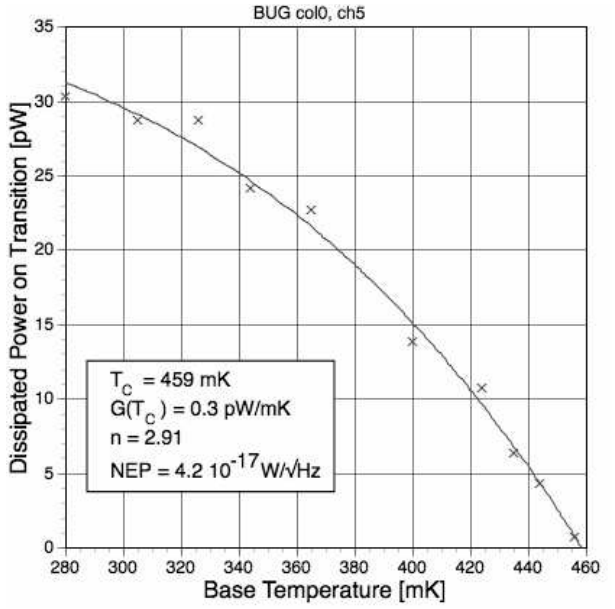


**Figure 9.** Plot showing a fit to the thermal conductivity of a suspended pixel of a 2x2 array versus base temperature. The derived device parameters are included in the figure.

We have developed a new type of 2-dimensional planar bolometer array architecture, which separates the array and the backshort production, allowing a straightforward way to provide bolometer arrays for a wide range of wavelengths[10]. A 8x16 Backshort Under Grid (BUG) array will be used in GISMO. Fig. 6 shows an image of an 8x8 BUG array fabricated in our group at NASA/GSFC. Fig. 7 presents an enlargement of one pixel which shows the integrated Transition Edge Sensor (TES) bolometer in more detail. The normal metal Zebra structure on the device, which is used to suppress excess noise[11], is clearly visible in this image. We have tested witness samples of the BUG devices. The quantitative results presented here were obtained from testing a pixel from a suspended 2x2 pixel array. Fig. 8 shows a representative I-V curve for a BUG device. Figure 9 shows the thermal conductivity of a suspended pixel of a 2x2 array versus base temperature. The device parameters derived from

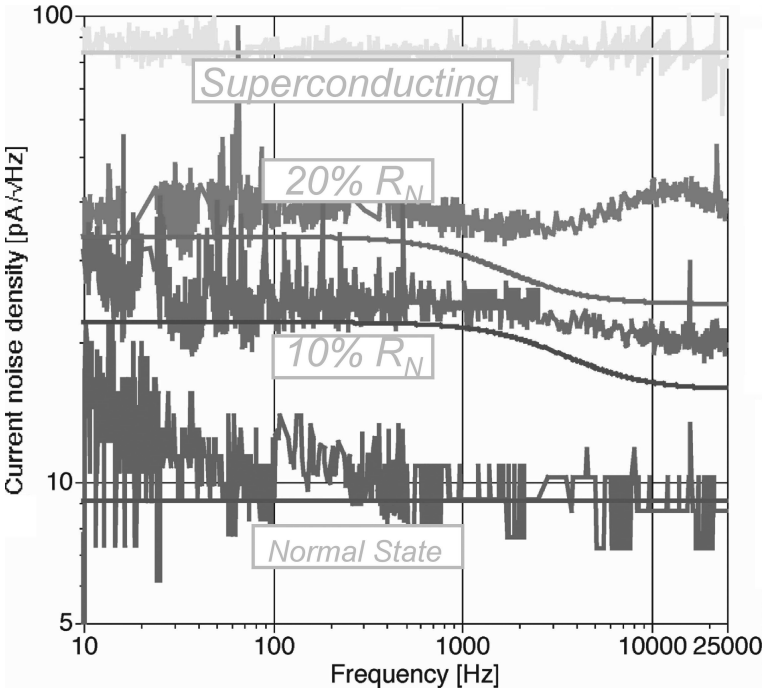


**Figure 10.** Noise spectrum of a BUG device in its superconducting state (top), on the transition (two bias points can be seen in the center of the graph), and in its normal state (bottom). Superimposed is the expected fundamental thermodynamic noise limit for the independently measured device parameters.

the fit are included in the figure. The phonon noise equivalent power (NEP) of the device is $4.2 \times 10^{-17}\mathrm{W}/\sqrt{\mathrm{Hz}}$, which will add about 25 percent to the expected sky noise of $9 \times 10^{-17}\mathrm{W}/\sqrt{\mathrm{Hz}}$ at 2 mm and 20% bandwidth during winter conditions at the site of the 30 m telescope. A reduction in the transition temperature (the tested device has $T_c$= 459 mK) could be used to further improve the detector noise without any modification of the array design, since GISMO will provide a base temperature that allows operation of TES with $T_c$ of $\sim$ 400 mK or slightly less), however we are not planning to do this at this time, because under mediocre weather conditions and lower elevations those detectors would saturate from the thermal emission from the sky. The tested device has an electro-thermal feedback time constant of about 50 $\mu$s ($f_{\mathrm{TES}} \sim 3.5$ kHz). The detector circuit contains a Nyquist inductor which is is chosen such that the detector integrates for a full readout cycle of the multiplexer (typically the frame rate is set to several tens of kHz). Fig. 10 shows the measured noise spectrum of this device in its superconducting state, on the transition (two bias points are shown), and in its normal state. Superimposed is the expected thermodynamic noise for the device, using the known values for the SQUID noise and the shunt resistor. The Nyquist L/R rolloff was removed in the plot in order to highlight the intrinsic device performance. The measured in-band noise of the device on both measured bias points is less than 20% above the fundamental phonon noise limit. Only the out-of-band excess noise is higher than this value. This noise will be suppressed by the Nyquist filter and therefore will not degrade the detector performance.

## 4. DEWAR, OPTICS, AND ELECTRONICS

A drawing of the dewar and the optics is shown in Fig. 11. The dewar has a combination of $^4$He and $^3$He evaporation coolers, which are assembled into the pocketed baseplate of the dewar, providing a base temperature of 260 mK for the detector array. A 110 mm wide anti-reflection coated silicon lens provides the required $f/1.2$ of the optics for a $\sim 0.9\lambda/D$ sampling, intended to optimize the efficiency of GISMO for large area blank sky surveys, without compromising the achievable point source signal-to-noise ratio. The silicon lens will be cooled to 4 K. The TES arrays are read out by four 32-channel SQUID multiplexers provided by NIST/Boulder[12]. Both the read out electronics[13] and the IRC control- and data acquisition software[14] are used in other instruments

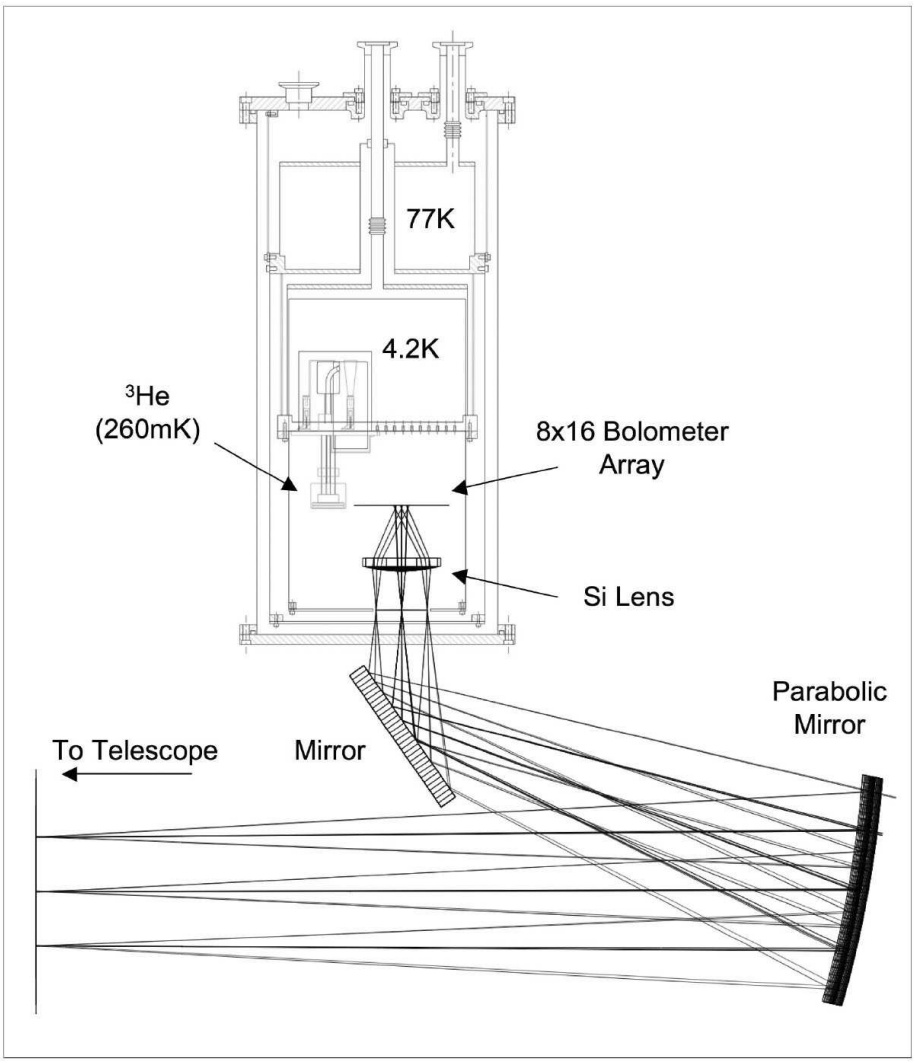


**Figure 11.** Simplified line drawing of the GISMO dewar, showing positions of key elements such as detector array and major optical components. The diameter of the cold plate is 10 inches.

such as the GBT 3 mm bolometer camera[15].

## REFERENCES

1. Baars, J. W. M.; Hooghoudt, B. G.; Mezger, P. G.; de Jonge, M. J., 1987, A&A, 175, 319
2. http://www.iram.es/IRAMES/otherDocuments/manuals/manual_v20.ps
3. Blain, A.W.; Smail, I.; Ivison, R.J.; Kneib, J.-P.; Frayer, D.T., 2002, PhR, 369, 111
4. Kreysa, E.; Gemnd, H.-P.; Raccanelli, A.; Reichertz, L. A.; Siringo, G., 2002, AIPC, 616, 262
5. Glenn, J.; Bock, J.J.; Chattopadhyay, G.; Edgington, S.F.; Lange, A.E.; Zmuidzinas, J.; Mauskopf, P.D.; Rownd, B.; Yuen, L.; Ade, P.A. 1998, SPIE, 3357, 326
6. Cunningham, C.R.; Gear, W.K., 1990, SPIE, 1235, 515
7. Holland, Wayne S.; Duncan, William; Kelly, B. D.; Irwin, Kent D.; Walton, Anthony J.; Ade, Peter A. R.; Robson, E. I., 2003, SPIE, 4855, 1
8. Bernstein, G., 2002, PASP, 114, 98

9. Willott, C. J., McLure, R. L., Jarvis, M. J., 2003, ApJ, 587, L15
10. Allen, C.A., Benford, D.K., Chervenak, J.A., Chuss, D.T., Miller,T.M., Moseley, S.H., Staguhn, J.G., Wollack, E.J., 2006, Nuclear Instruments and Methods in Physics Research, Section A (NIMPA), 559, 522
11. Staguhn, J.G., Benford, D.J., Chervenak, J.A., Moseley, S.H., Jr., Allen, C.A.; Stevenson, T.R.; Hsieh, W-T., 2004, SPIE, 5498, 390
12. de Korte, P.A. J.; Beyer, J.; Deiker, S.; Hilton, G.C.; Irwin, K.D.; Macintosh, M.; Nam, S.W.; Reintsema, C.D.; Vale, L. R.; Huber, M.E., 2003, RScI, 74. 3807
13. Forgione, J.B.; Benford, D.J.; Buchanan, E.D.; Moseley, S. H., Jr.; Rebar, J.; Shafer, R.A., 2004, SPIE, 5498, 784
14. Ames, T. J.; Case, L., 2003, SPIE, 4857, 73
15. Benford, D.J., Dicker, S.R., Wollack, E.J., Supanich, M.P., Staguhn, J.G., Moseley, S.H., Irwin, K.D., Devlin, M.J., Chervenak, J.A., Chen, T.C. , 2004, SPIE, 5498, 208